

Supporting Information

**Reversal of a Single Base-Pair Step Controls Guanine Photo-Oxidation
by an Intercalating Ruthenium(II) Dipyridophenazine Complex****

Páraic M. Keane, Fergus E. Poynton, James P. Hall, Igor V. Sazanovich, Michael Towrie,
Thorfinnur Gunnlaugsson, Susan J. Quinn, Christine J. Cardin,* and John M. Kelly**

anie_201502608_sm_miscellaneous_information.pdf

Experimental

1. Materials	S2
2. Steady-state spectroscopy	S2
3. Transient spectroscopy – psTA and ps/ns-TRIR	S2

Figures and Tables

Figure S1: Complex intercalated at G ₉ G ₁₀ ;C ₁ C ₂ from structure of Λ -[Ru(phen) ₂ (dppz)] ²⁺ in the presence of {CCGG <u>A</u> TCCGG} ₂ , showing selected distances.	S4
Figure S2: Complex intercalated at T ₅ A ₆ ;T ₅ A ₆ from structure of Λ -[Ru(phen) ₂ (dppz)] ²⁺ in the presence of {CCGG <u>T</u> ACCGG} ₂ , showing selected distances.	S4
Figure S3: Ps/Ns-TA spectra of Λ -[Ru(TAP) ₂ (dppz)] ²⁺ in the presence of (a) {CCGG <u>A</u> TCCGG} ₂ , ODN A ; (b) CCGG <u>T</u> ACCGG ₂ , ODN B .	S5
Figure S4: TRIR spectra of Λ -[Ru(TAP) ₂ (dppz)] ²⁺ in presence of (a) {CCGG <u>A</u> TCCGG} ₂ (ODN A) and (b) {CCGG <u>T</u> ACCGG} ₂ (ODN B) showing region where metal complex absorbs.	S6
Figure S5: TRIR spectra of Λ -[Ru(TAP) ₂ (dppz)] ²⁺ in presence of {CCGG <u>A</u> TCCGG} ₂ (ODN A), showing evolution of spectra with time.	S7
Figure S6: TRIR spectra of Λ -[Ru(TAP) ₂ (dppz)] ²⁺ in the presence of poly{dAdT} ₂	S7
Figure S7: Comparative TRIR spectra for Λ -[Ru(TAP) ₂ (dppz)] ²⁺ in presence of (a) ODN B vs poly{dAdT} ₂ (b) ODN B vs ODN A .	S8
Figure S8: UV/visible titrations of Λ -[Ru(TAP) ₂ (dppz)] ²⁺ in the presence of increasing concentrations of (a) ODN A , {CCGG <u>A</u> TCCGG} ₂ (b) ODN B , {CCGG <u>T</u> ACCGG} ₂ with corresponding fits to the Bard model.	S9
Figure S9: Changes in the emission spectra of Λ-1 with increasing additions of (a) ODN A (b) ODN B in 50 mM phosphate buffer (pH 7) Insert: Plot of (I _a -I _f)/(I _b -I _f) at 630 nm vs. [DNA] (M, nucleotide) using data with a Nuc : Ru ratio between 0-100 and the best fit using the Bard equation.	S10
Figure S10: CD spectra of Λ -[Ru(TAP) ₂ (dppz)] ²⁺ , native ODNs, and complex bound to ODN (Nuc:Ru = 25) for systems containing (a) ODN A (b) ODN B	S11
Table S1: Binding parameters for Λ -[Ru(TAP) ₂ (dppz)] ²⁺ in the presence of ODNs A and B	S10

1. Materials

Λ -[Ru(TAP)₂(dppz)]²⁺ was synthesized as recently described^[1] using a variation of literature methods.^[2,3,4] Oligonucleotides d{CCGGATCCGG} and d{CCGGTACCGG} were synthesized, desalted and purified (by gel filtration) by ATDBio Ltd (Southampton, UK). Extinction coefficients (single-stranded) of 91,800 M⁻¹cm⁻¹ and 92,200 M⁻¹cm⁻¹ (260 nm) were used for d{CCGGATCCGG} and d{CCGGTACCGG} respectively. Poly{dAdT}₂ was purchased from Sigma-Aldrich ($\epsilon_{260} = 6600 \text{ M}^{-1}\text{cm}^{-1}$ per nucleotide).

2. Steady-state experiments

Circular dichroism (CD) experiments were recorded on a JASCO 810 spectropolarimeter. Ground-state binding studies were performed in 0.5 cm quartz cuvettes using a Cary 50 UV/visible spectrophotometer and Cary Varian Eclipse spectrofluorimeter. Binding constants were obtained by fitting to the model of Bard^[5] as follows:

$$(\epsilon_a - \epsilon_f) / (\epsilon_b - \epsilon_f) = (a - (a^2 - 2K^2[\text{Ru}][\text{DNA}]/a)^{1/2}) / 2K[\text{Ru}] ; a = 1 + K[\text{Ru}] + (K[\text{DNA}]/2s)$$

Where ϵ_a , ϵ_b and ϵ_f are the apparent, bound and free molar absorptivities, respectively; K is the association constant and s is the binding site size. For binding constants derived from luminescence experiments, ϵ was substituted with I, the luminescence intensity at 630 nm. Quantum yields of Λ -[Ru(TAP)₂(dppz)]²⁺ and ODN-bound complexes were determined using [Ru(bpy)₃]²⁺ as a standard.

3. Transient spectroscopy – psTA and ps/ns-TRIR

The samples for transient spectroscopy measurements were prepared in 50 mM potassium phosphate buffered (pH 7) D₂O. A known volume of solution (25 μ L) was dropped between two CaF₂ (25 mm diameter) windows (Crystran Ltd, UK), separated by a Teflon spacer of 50 μ m path length, in a demountable solution IR cell (Harrick Scientific Products Inc., New York).

Transient spectroscopic measurements were performed using the ULTRA and TR^MPS apparatus at the Central Laser Facility (Harwell, UK), which have been described in detail elsewhere.^[6,7] Ps-TrA measurements were recorded on ULTRA using identical conditions to those reported recently.^[1,8]

The TrA spectrometer comprises of a 10 kHz repetition rate titanium sapphire amplifier (Thales), producing 0.8 mJ output with 40 fs pulse duration, at 800 nm. The

second harmonic generation of the 800 nm created the 400 nm femtosecond pump pulses used in these experiments. The polarization of the pump pulses at the sample was at the magic angle relative to the probe, with an energy of 1 μJ . The 400 nm pump beam was mechanically chopped down to 5 kHz, focused ($\sim 100 \mu\text{m}$ spot sizes) and overlapped with the probe beam ($\sim 80 \mu\text{m}$ spot size) in the sample cell. Part of the titanium sapphire laser output beam was used to generate a white light continuum (WLC) in a CaF_2 plate. The crystal plate was continuously rastered to avoid color centre formation and to improve stability in the probe. The WLC was dispersed through the grating monochromator and detected using a linear silicon array (Quantum Detectors). In front of the monochromator, a 400 nm notch filter was placed in order to remove scatter from the excitation beam. The spectra were calibrated using five band-pass filters.

Ns-TrA and ps/ns-TRIR spectra were recorded using the Time-Resolved Multiple Probe Spectroscopy approach (hereafter TR^MPS)^[7], as described recently.^[1]

In the TR^MPS configuration, another 1 kHz titanium sapphire amplifier (Spectra Physics Spitfire XP) was used to produce the excitation beam (100 fs, 400 nm after frequency doubling, pulse energy at sample attenuated down to 1 μJ and focused down to $100 \times 200 \mu\text{m}^2$ spot). For the probe the same 10 kHz ULTRA laser beam was used as described above. Both ULTRA amplifier and Spitfire amplifier were synchronized by sharing the same seed from 68 MHz titanium sapphire oscillator. The seed beam was delayed with an optical delay line before the 1 kHz amplifier to accommodate for 100 fs – 14.7 ns time delays between pump and probe. To go beyond 14.7 ns up to 100 μs , subsequent seed pulses were selected from the 68 MHz seed pulse train accompanied by the appropriate setting of the optical delay line. The sequence of the probe pulses arriving to the sample (at 10 kHz repetition rate) probes the transient absorption of the sample on the time up to 1 ms (when the following pump pulse arrives) with an interval of 100 μs .

The polarization of the excitation beam at the sample was set to be at the magic angle with respect to the probe. Samples for TRIR and TrA experiments were raster scanned in the x and y directions to minimize photodamage and re-excitation effects. Samples were checked before and after the experiment by UV/vis spectroscopy.

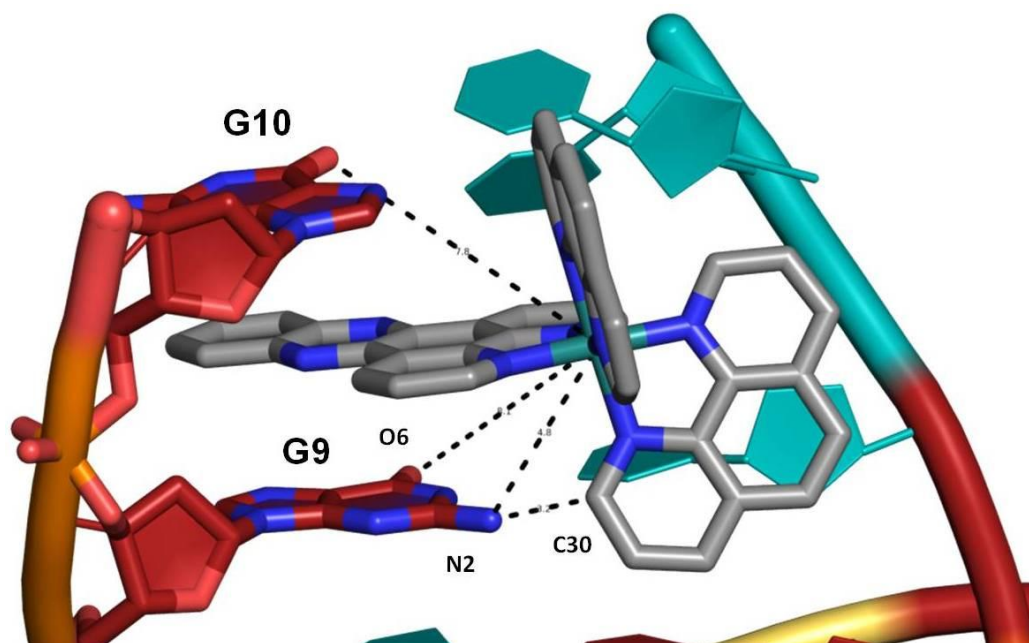


Figure S1: Complex intercalated at G₉G₁₀;C₁C₂ from structure of Λ -[Ru(phen)₂(dppz)]²⁺ in the presence of {CCGGATCCGG}₂,^[9] showing selected distances:

Ru – N2(G9) = 4.8 Å
 Ru – O6 (G9) = 8.1 Å
 Ru – O6 (G10) = 7.8 Å
 phen(C30)-N2(G9) = 3.1 Å

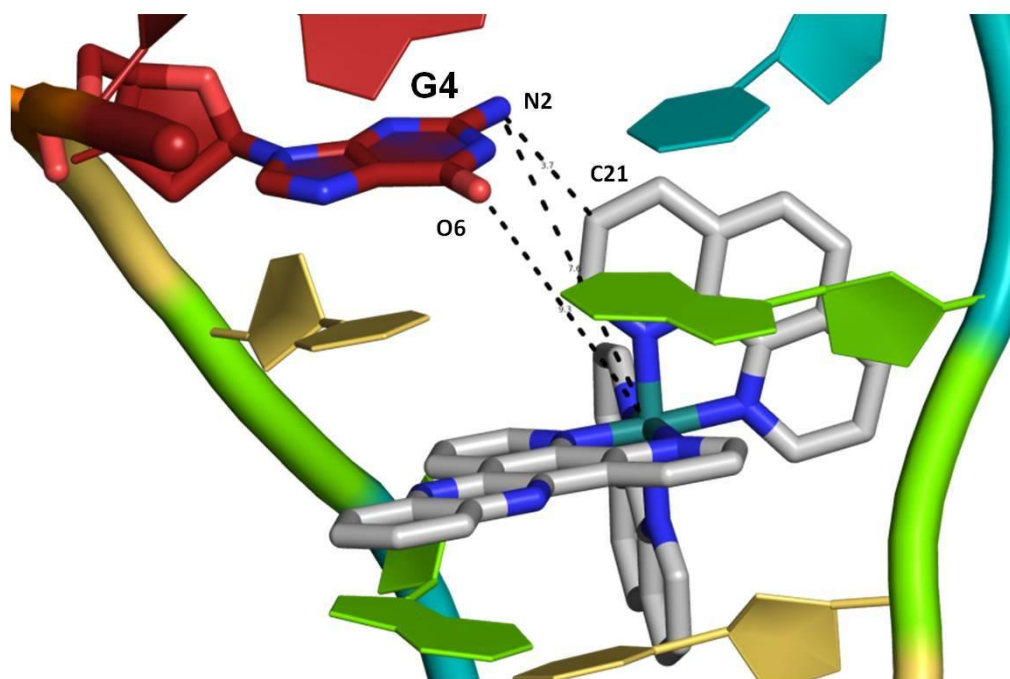


Figure S2: Complex intercalated at T₅A₆;T₅A₆ from structure of Λ -[Ru(phen)₂(dppz)]²⁺ in the presence of {CCGGTACCGG}₂,^[9] showing selected distances:

Ru – N2(G4) = 7.6 Å
 Ru – O6 (G4) = 9.3 Å
 phen(C21) – N2(G4) = 3.7 Å

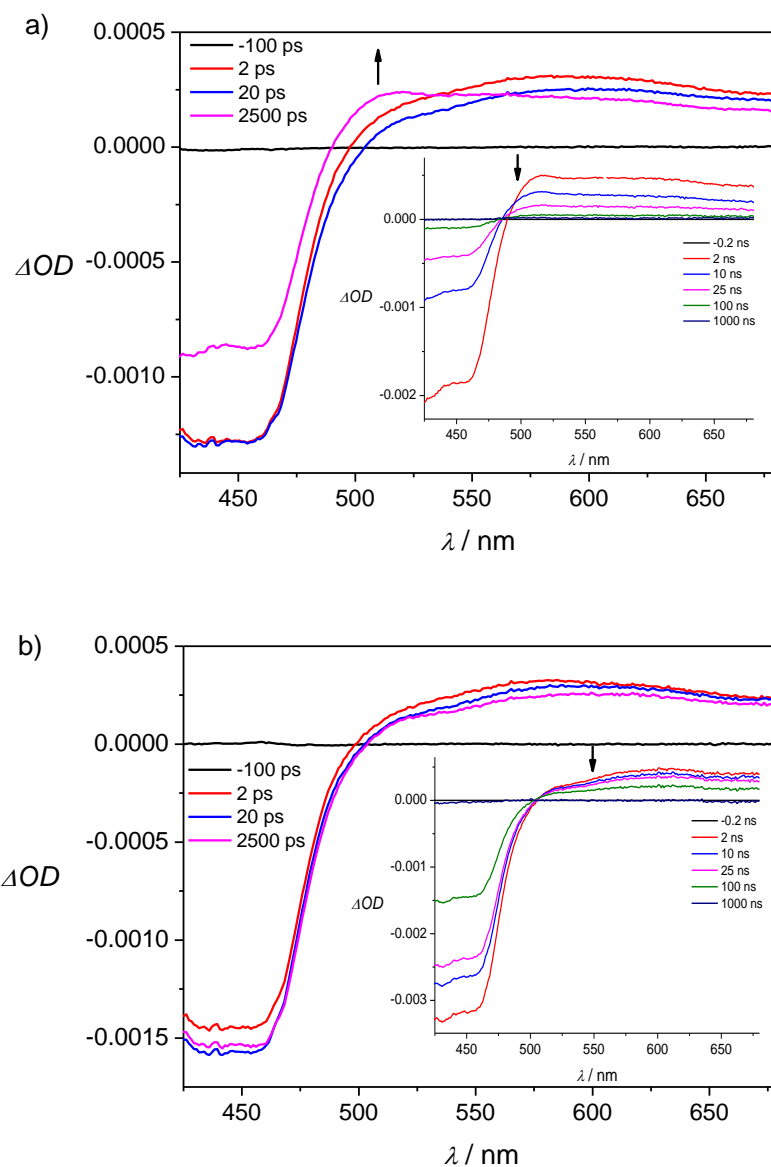


Figure S3: Ps/Ns-TA spectra of 400 μM Λ -[Ru(TAP)₂(dppz)]²⁺ in the presence of (a) {CCGGATCCGG}₂, ODN **A**; (b) CCGGTACCGG}₂, ODN **B**. Shown at selected delays. Ns-TA spectra shown as insets. $\lambda_{\text{exc}} = 400 \text{ nm}$, 1 μJ , 100 fs

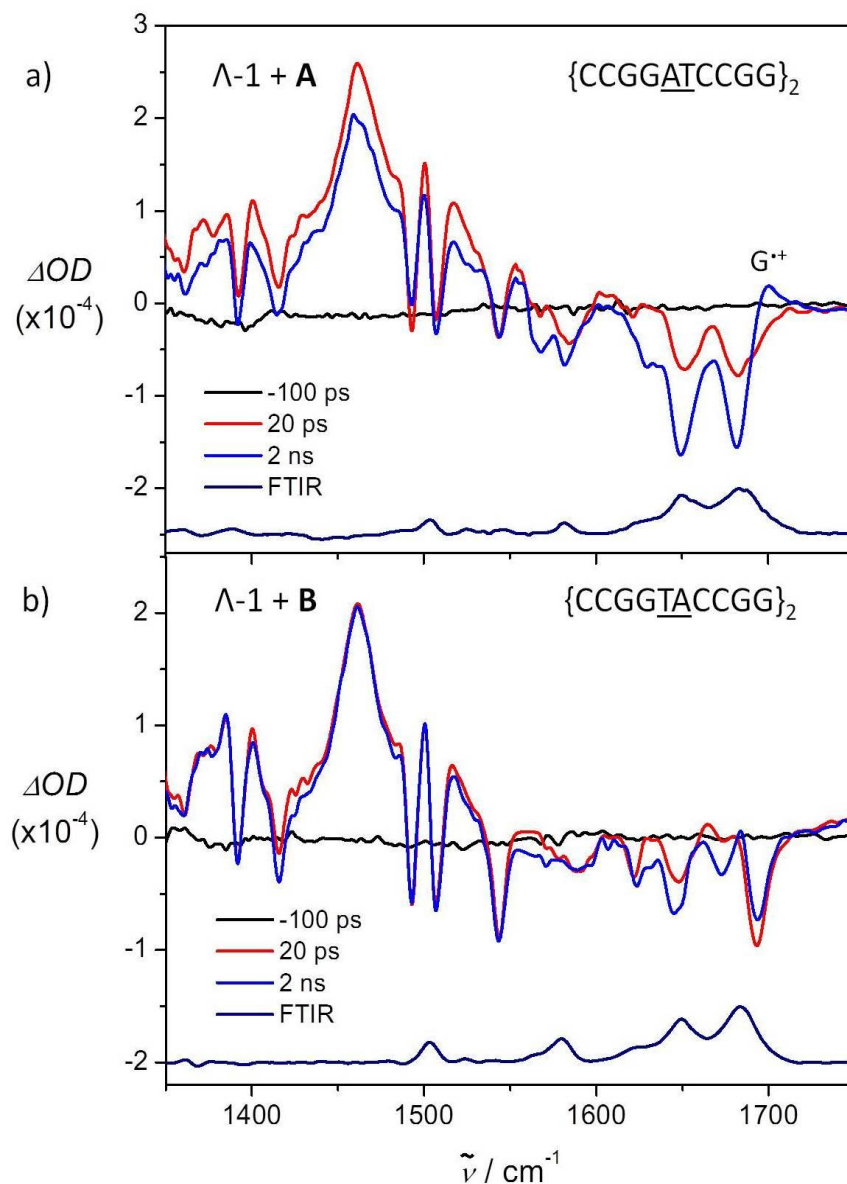


Figure S4: TRIR spectra of Λ -[Ru(TAP)₂(dppz)]²⁺ in the presence of Λ -[Ru(TAP)₂(dppz)]²⁺ in presence of (a) {CCGGATCCGG}₂ (ODN A) and (b) {CCGGTACCGG}₂ (ODN A), showing region where vibrations of the metal complex appear (< ~1600 cm⁻¹) as well as region of DNA nucleobase vibrations (>~ 1600 cm⁻¹). $\lambda_{\text{exc}} = 400 \text{ nm}$, 1 μJ , 100 fs

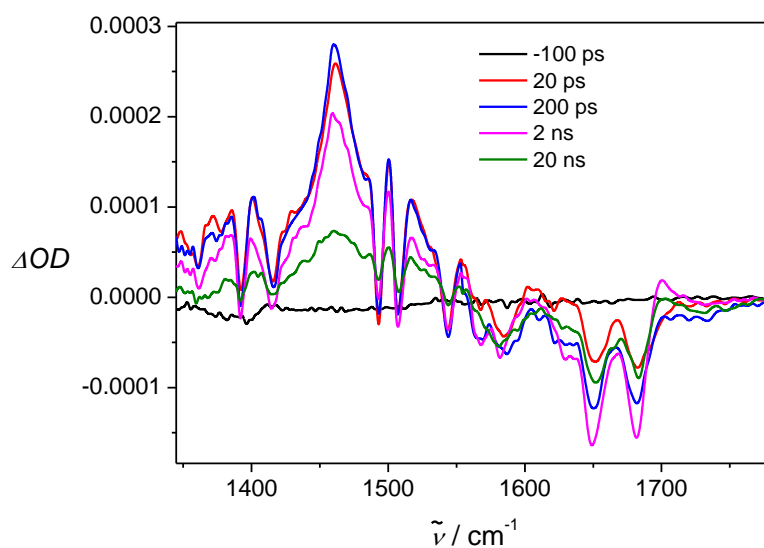


Figure S5: TRIR spectra of Λ -[Ru(TAP)₂(dppz)]²⁺ in the presence of {CCGGATCCGG}₂ (ODN A), showing evolution of spectra with time. $\lambda_{\text{exc}} = 400 \text{ nm}$, $1 \mu\text{J}$, 100 fs

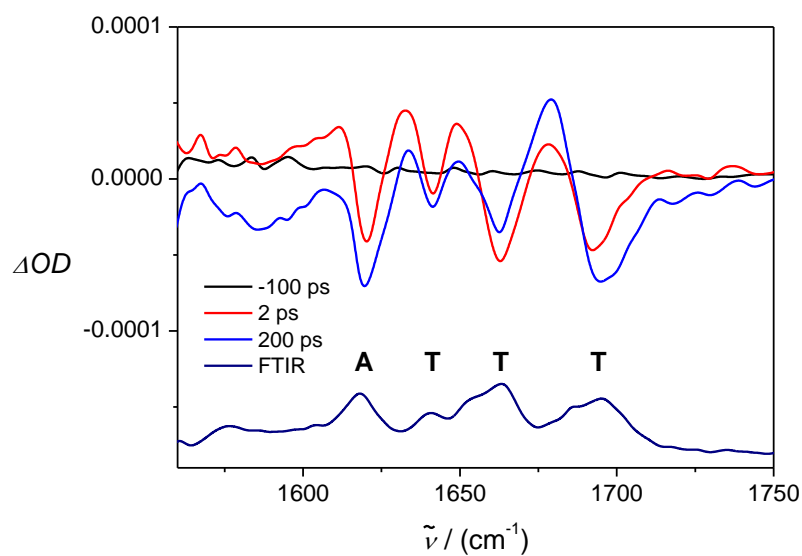


Figure S6: $400 \mu\text{M}$ Λ -[Ru(TAP)₂(dppz)]²⁺ in the presence of poly{dAdT}₂ (8 mM nucleotide; P/D = 20). $\lambda_{\text{exc}} = 400 \text{ nm}$, $1 \mu\text{J}$, 100 fs

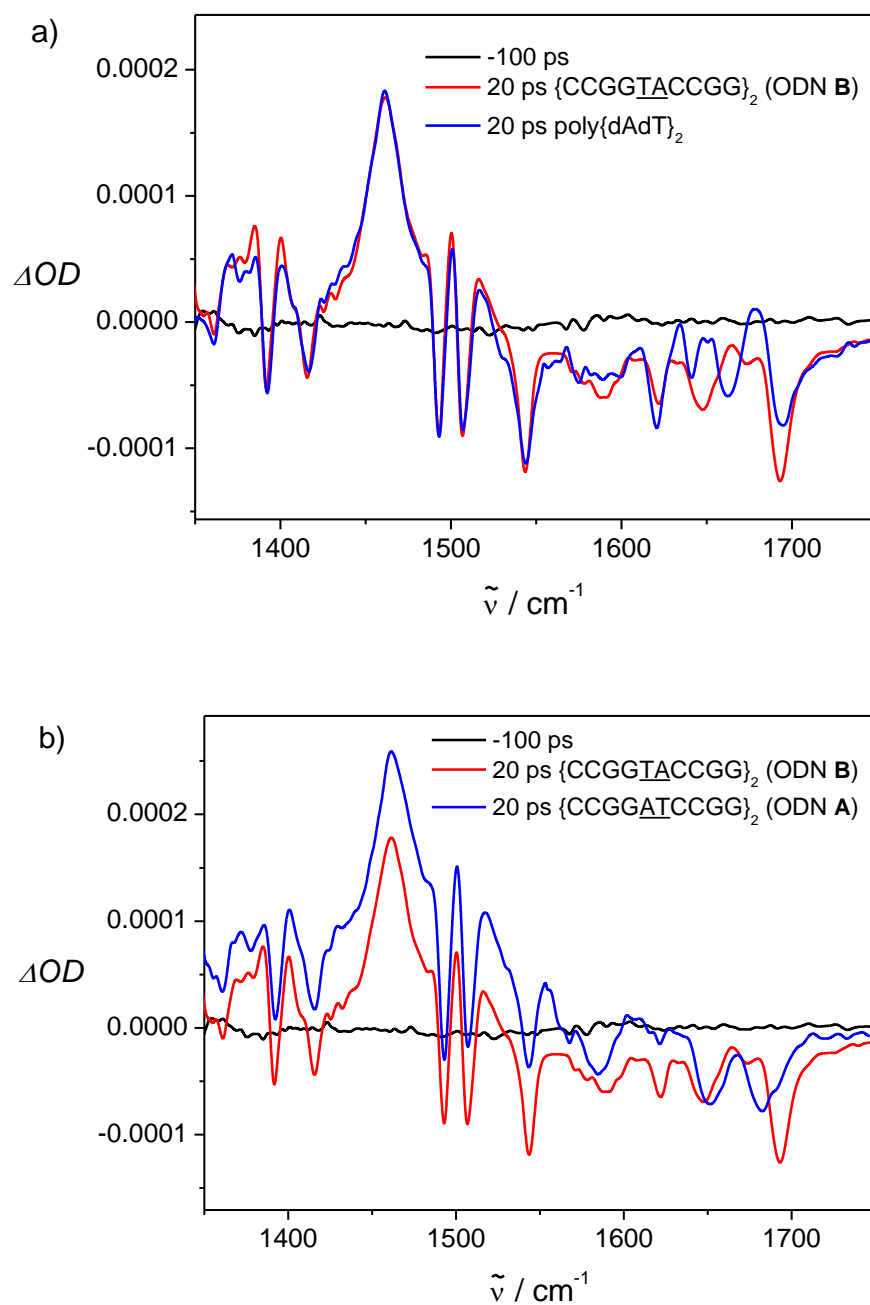


Figure S7: Comparative TRIR spectra at 20 ps for 400 μM $\Lambda\text{-}[\text{Ru}(\text{TAP})_2(\text{dppz})]^{2+}$ in presence of (a) ODN **B** vs poly{dAdT}₂ (b) ODN **B** vs ODN **A**. $\lambda_{\text{exc}} = 400 \text{ nm}$, 1 μJ . [ODN] = 500 μM duplex. [poly{dAdT}₂] = 8 mM nucleotide; P/D = 20.

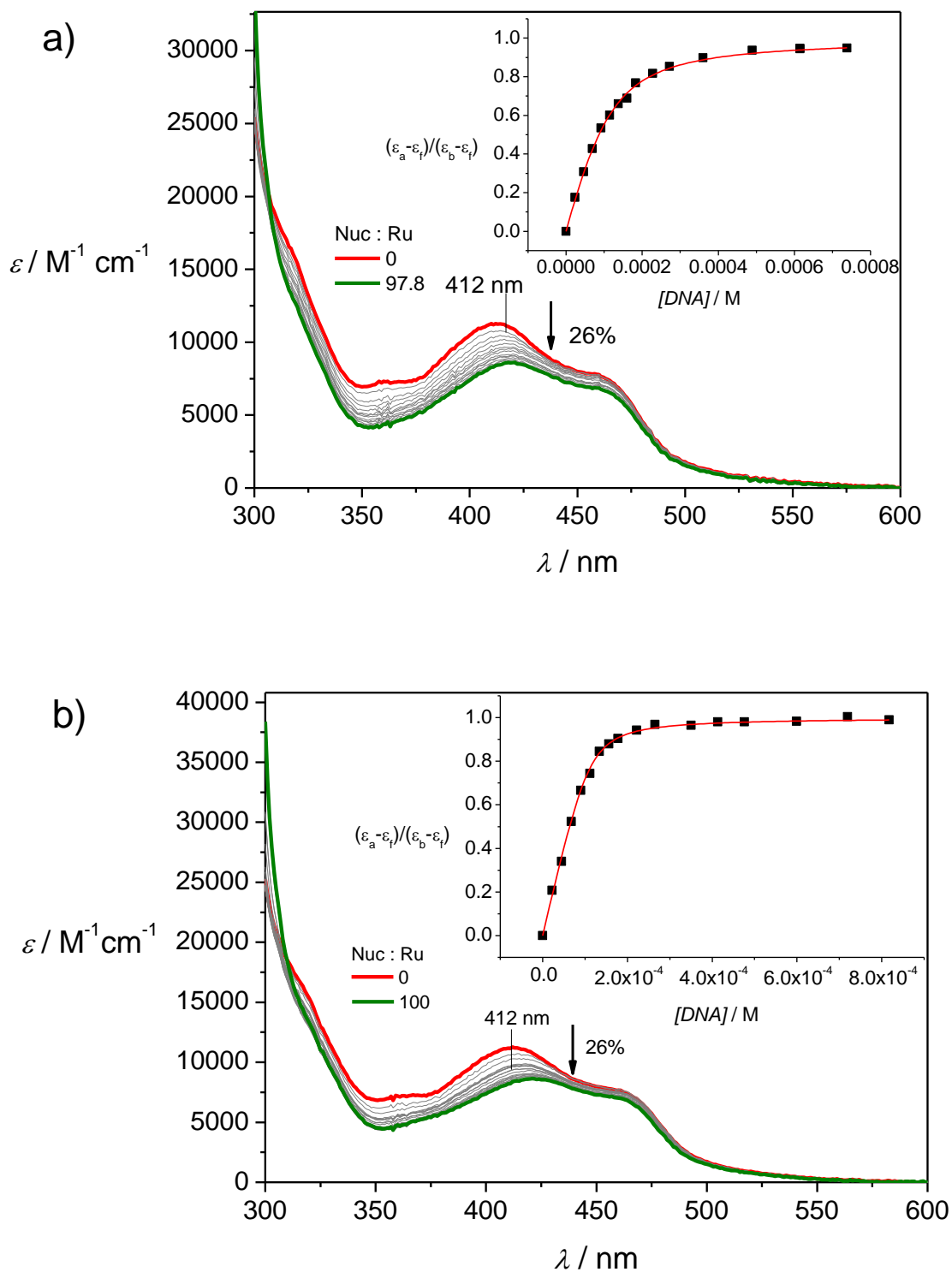


Figure S8: UV/visible titrations of Λ -[Ru(TAP)₂(dppz)]²⁺ (8.8 μ M) in the presence of increasing concentrations of (a) ODN **A**, {CCGGATCCGG}₂ (b) ODN **B**, {CCGGTACCGG}₂. Insets show fits to Bard model^[5] from absorbance changes monitored at 412 nm. In 50 mM phosphate buffer in H₂O, pH 7.

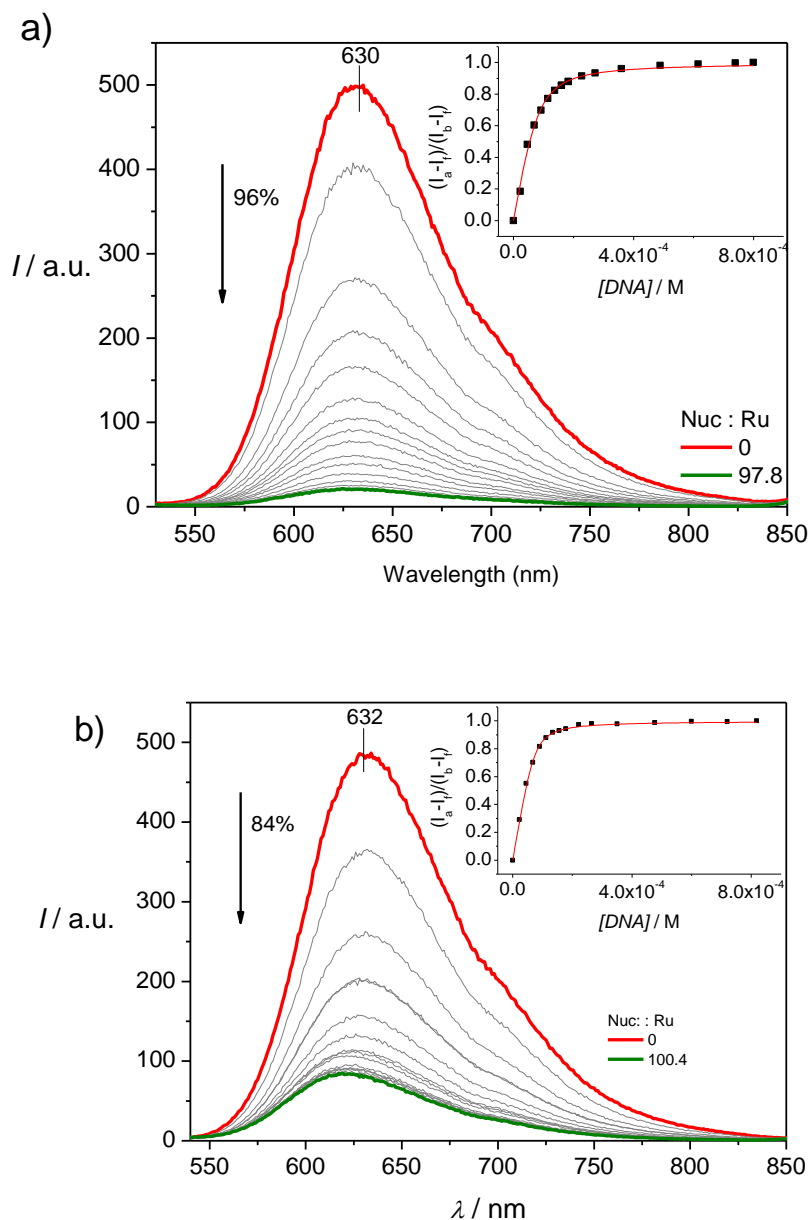


Figure S9: Changes in the corrected emission spectrum of Λ -1 (8.8 μM , $\lambda_{\text{ex}} = 435$ nm) with increasing additions of (a) {CCGGATCCGG}₂, ODN **A** (b) {CCGGTACCGG}₂, ODN **B** (0 – 44.9 μM duplex) in H₂O (50 mM phosphate buffer; pH 7) at 298 K. Inset: Plot of $(I_a - I_f)/(I_b - I_f)$ at 630 nm vs. [DNA] (M, nucleotide) using data with a Nuc : Ru ratio between 0-100 and the best fit of the data (---) using the Bard model.^[5] *Decreased emission quenching in ODN B is indicative of less efficient ET*

Table S1: Binding parameters for Λ -[Ru(TAP)₂(dppz)]²⁺ in the presence of ODNs **A** and **B**. ^ahypochromism at 420 nm. ^bdetermined from UV/vis spectra ^cerror is $\pm 10\%$, quantum yield for unbound Λ -1 determined as 0.035 ± 0.004 . ^ddetermined from emission spectra

ODN	H ^a	K ^b (M ⁻¹)	R ²	Φ_f^c	K ^d (M ⁻¹)	R ²
{CCGGATCCGG} ₂	26%	$(3.5 \pm 0.4) \times 10^5$	0.99	0.001	$(6.2 \pm 0.9) \times 10^5$	0.99
{CCGGTACCGG} ₂	26%	$(1.6 \pm 0.2) \times 10^6$	0.99	0.005	$(1.3 \pm 0.1) \times 10^6$	0.99

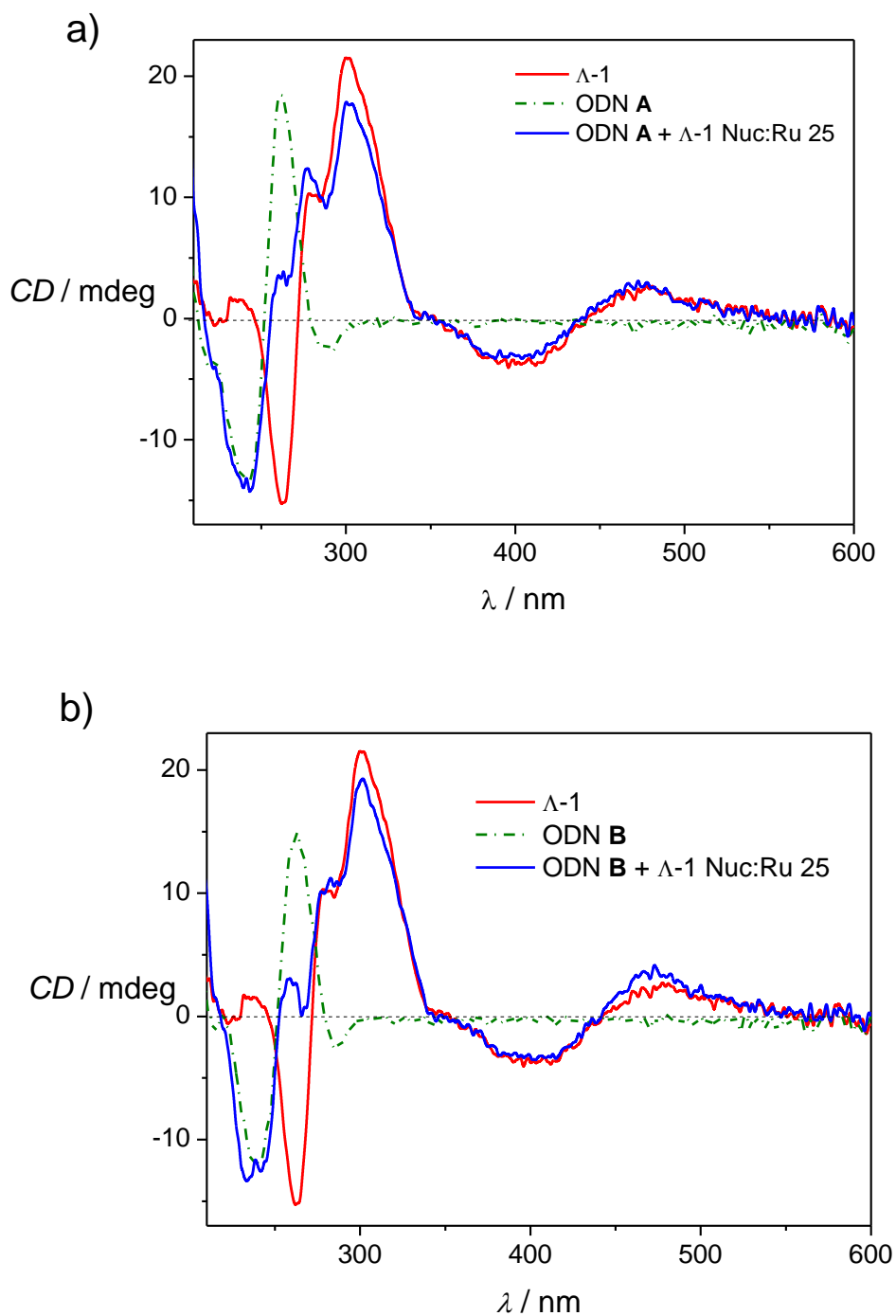


Figure S10: The circular dichroism spectra of Λ -[Ru(TAP)₂(dppz)]²⁺ (8.8 μ M, red), native ODNs (11 μ M, olive) and complex bound to ODN (Nuc:Ru = 25, blue) for systems containing (a) ODN **A** (b) ODN **B** in H₂O in potassium phosphate buffer (50 mM, pH 7) at 298 K. *Interpretation of the CD spectra is complicated by overlapping bands from both ODN and Ru complex. Spectra show a similar structure for either ODN*

References

1. P. M. Keane, F. E. Poynton, J. P. Hall, I. P. Clark, I. V. Sazanovich, M. Towrie, T. Gunnlaugsson, S. J. Quinn, C. J. Cardin, J. M. Kelly, *J. Phys. Chem. Lett.* **2015**, *6*, 734-738.
2. I. Ortmans, B. Elias, J. M. Kelly, C. Moucheron, A. Kirsch-DeMesmaeker, *Dalton Trans.* **2004**, 668-676.
3. S. Vasudevan, J.A. Smith, M. Wojdyla, A. di Trapani, P.E. Kruger, T. McCabe, N. C. Fletcher, S. J. Quinn, J. M. Kelly, *Dalton Trans.* **2010**, *39*, 3990-3998.
4. K. O'Sullivan, Ph.D. Thesis, University of Dublin **2011**.
5. M. T. Carter, M. Rodriguez, A. J. Bard, *J. Am. Chem. Soc.* 1989, **111**, 8901-8911.
6. G. M. Greetham, P. Burgos, Q. Cao, I. P. Clark, P. S. Codd, R. C. Farrow, M. W. George, M. Kogimtzis, P. Matousek, A. W. Parker, M. R. Pollard, D. A. Robinson, Z. J. Xin, M. Towrie, *Appl. Spectrosc.* **2010**, *64*, 1311-1319.
7. G. M. Greetham, D. Sole, I. P. Clark, A. W. Parker, M. R. Pollard, M. Towrie, *Rev. Sci. Instrum.* **2012**, *83*, 103107
8. S. J. Devereux, P. M. Keane, S. Vasudevan, I. V. Sazanovich, M. Towrie, Q. Cao, X.-Z. Sun, M. W. George, C. J. Cardin, N. A. P. Kane-Maguire, J. M. Kelly, S. J. Quinn, *Dalton Trans.* **2014**, *43*, 17606-17609.
9. H. Niyazi, J. P. Hall, K. O'Sullivan, G. Winter, T. Sorensen, J. M. Kelly, C. J. Cardin, *Nat. Chem.* **2012**, *4*, 621-628.

Article references with full author lists

- 5c) J. P. Hall, D. Cook, S. R. Morte, P. McIntyre, K. Buchner, H. Beer, D. J. Cardin, J. A. Brazier, G. Winter, J. M. Kelly, C. J. Cardin, *J. Am. Chem. Soc.* **2013**, *135*, 12652-12659.
- 7c) B. Elias, C. Creely, G. W. Doorley, M. M. Feeney, C. Moucheron, A. Kirsch-De Mesmaeker, J. Dyer, D. C. Grills, M. W. George, P. Matousek, A. W. Parker, M. Towrie, J. M. Kelly, *Chem. Eur. J.* **2008**, *14*, 369-375.
- 8a) G. M. Greetham, P. Burgos, Q. Cao, I. P. Clark, P. S. Codd, R. C. Farrow, M. W. George, M. Kogimtzis, P. Matousek, A. W. Parker, M. R. Pollard, D. A. Robinson, Z. J. Xin, M. Towrie, *Appl. Spectrosc.* **2010**, *64*, 1311-1319.
- 10) Q. Cao, C. M. Creely, J. Dyer, T. L. Easun, D. C. Grills, D. A. McGovern, J. McMaster, J. Pitchford, J. A. Smith, X.-Z. Sun, J. M. Kelly, M. W. George, *Photochem. Photobiol. Sci.* **2011**, *10*, 1355-1364.